Received: 12 July 2019 | Revised: 14 November 2019 | Accepted: 3 December 2019

DOI: 10.1002/pip.3234

EU PVSEC PAPER

PROGRESS IN PHOTOVOLTAICS WILEY

Power performance and thermal operation of organic photovoltaic modules in real operating conditions

Giorgio Bardizza[1] | Elena Salis[1] | Carlos Toledo[2] | Ewan D. Dunlop[1]

[1]European Commission, Joint Research Centre (JRC), Ispra, Italy

[2]Department of Electronics, Computer Technology and Projects, Technical University of Cartagena, Cartagena, Spain

Correspondence
Giorgio Bardizza, European Commission, Joint Research Centre (JRC), Ispra, Italy.
Email: giorgio.bardizza@ec.europa.eu

Abstract

Printed organic photovoltaics (OPVs) have moved beyond the research laboratory phase and have demonstrated their suitability to be upscaled for industrial manufacture. The improved efficiencies and increased lifetime testify the potential for this technology to compete with crystalline silicon–based technologies under some operating conditions. There are companies capable of producing large-area OPV modules for outdoor installation. Examples of solar cell production on an industrial scale for energy production have been shown in the last 5 years. In this work, we present the performance data of a large-area OPV module under operating conditions representative for real outdoor operation. This study focuses on the analysis of the thermal behavior of the module and shows how its performance can be affected by the temperatures it can reach outdoor under natural sunlight. A comparison of outdoor measurements with indoor data measured under simulated sunlight at several temperature-irradiance combinations is also presented.

KEYWORDS

OPV, organic photovoltaics, photovoltaics, power measurements, power rating, temperature coefficients

1 | INTRODUCTION

Emerging photovoltaic (PV) technologies are rapidly evolving, and considerable research effort has addressed alternative approaches to increase their efficiency, reaching in the last years promising values.[1] A reliable technology assessment and a correct evaluation of their potential when compared with currently available PV technologies require performance measurements of the PV modules not only at standard test conditions (STCs) but also at real operating conditions (IEC 61853-1).[2] The aim of this study is to provide an insight into the performance of a recent commercial full-size organic PV (OPV) module measured under real operation conditions. This is also prerequisite to allow subsequent energy-rating studies and energy performance evaluation at different locations and climate conditions according to the IEC 61853 series, as already shown in the recent past.[3]

Only a few examples of large-area OPV modules are available in the world, and their study is fundamental to increase the confidence and reliability of these products and prototypes toward their marketability. There are examples of medium-term (2 years) outdoor operation through a large-scale, grid-tied, high-voltage system showing that thin plastic foil can be operated as an energy-producing technology.[4] In our study, a more detailed characterization of one large-area OPV module carried out at different temperature-irradiance conditions is reported, and preliminary data from its outdoor monitoring under natural sunlight are shown. A full power matrix of the OPV module under test was initially performed indoor

by measuring I-V curves at a continuous large-area solar simulator at the European Solar Test Installation (ESTI) of the European Commission. The electrical parameters' dependence on temperature is analyzed in detail, including evaluating its deviation from the straight-line function according to IEC 60904-10.[5] A polynomial fit is used instead to describe the dependence of P_{max} with T at different irradiance levels and build a power matrix according to IEC 61853-1. Finally, preliminary data acquired monitoring the device mounted outdoor under natural sunlight in our energy-rating (ENRA) system are shown. The discussion is focused on the temperature dependence of V_{oc} and I_{sc} at one selected irradiance as example. A comparison with the data measured indoor is also presented and discussed.

2 | EXPERIMENTAL

2.1 | Device under test

One roll-to-roll printed large-area OPV module provided by an external company was the device under test (DUT, ESTI code: TK801). The module has a total area of 0.72 m^2 and an active device area of 25 × 195 cm^2. It is made of 24 cells serially connected and was provided already mounted on a rigid metallic frame and with MC4 connectors. An STC calibration was performed at the beginning according to the standard IEC 60904-1[6] and those results are reported in a previous work.[7] The nominal high V_{oc} value could suggest this device to be a double-junction device according to the typical values expected for this technology. Therefore, we performed a deep investigation by several spectral responsivity measurements at different bias conditions (including the dark). However, none of them did confirm the multi-junction nature of the device. The DUT behaved as a single-junction device and therefore was treated as such.

2.2 | Indoor power matrix

I-V curves of TK801 were measured under indoor controlled conditions, at different levels of irradiance and module temperatures. A class AAA (IEC 60904-9)[8] large-area continuous solar simulator was used as light source. More details about the solar simulator can be found in Salis et al.[9] The irradiance level has been controlled by opening and closing the shutters placed in front of the 11 lamps of the simulator. The module was cooled down to about 10 °C prior to electrical measurements with the use of a temperature-controlled climatic chamber and allowed to naturally warm up under illumination. The module temperature was measured by a Pt100 sensor attached to the rear side of the module and close to its center. The unavoidable temperature raise over one I-V scan varies with the irradiance and temperature levels. The maximum variation was reached at 1000 W/m^2 and 15 °C and was 0.7 °C. Care was taken in eliminating the condensed water vapor prior to the start of the measurements, which were effectively initiated at a temperature just above the dew point.

Periodical I-V measurements were acquired during the warm-up of the module spanning the temperature range 15 °C to 55 °C for fixed irradiance and at temperature intervals of 5 °C. The measurements were performed at irradiances close to the nominal values of (1000, 800, 600, 400, 200, 100) W/m^2 and corrected afterwards to the nominal irradiances. The main electrical parameters V_{oc}, I_{sc}, FF, and P_{max} were extracted from the I-V curves and analyzed. In this work, we present the variation of V_{oc}, I_{sc}, and P_{max} in the measured range of temperature and irradiance.

2.3 | Outdoor measurements

After indoor initial characterization, the DUT was installed outdoor at ENRA. The ENRA system consists of a fixed south-facing rack, 36° tilted and located at 45°48′42.1″ North and 008°37′36.3″ East. The in-plane irradiance was measured with two different calibrated reference devices, suitable for permanent outdoor mounting: a c-Si ESTI sensor[10] and a pyranometer. Both ambient and module temperatures were measured by Pt100 temperature sensors: one was mounted in a shielded housing for ambient temperature, while two sensors were attached with aluminum tape onto the rear side of the module and the average value of their readings was then used. The wind speed and direction were measured using an ultrasound anemometer with analog outputs. All these environmental data and the TK801 I-V curve were simultaneously measured daily every 5 minutes from 06:00 (UTC + 1) to 20:00 (UTC + 1) whenever the irradiance was higher than

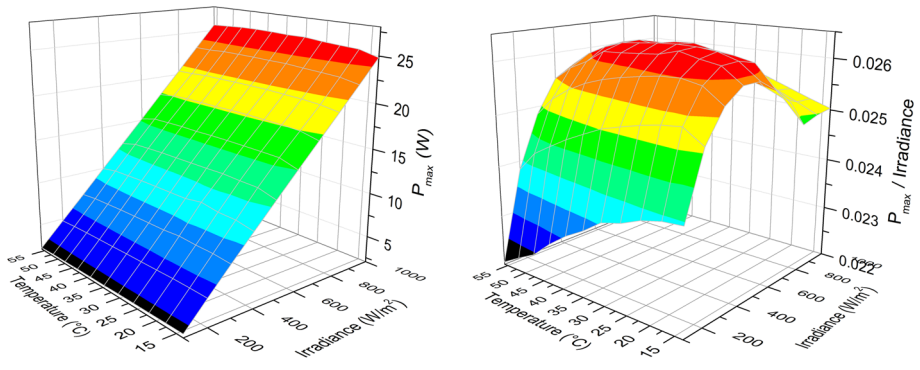

FIGURE 1 Power matrix data extracted from I-V curves measured at different temperature-irradiance combinations. Maximum power (left) and ratio between P_{max} and irradiance (right) are shown respectively in the two plots. Note that the ratio between P_{max} and irradiance is directly proportional to the efficiency [Colour figure can be viewed at wileyonlinelibrary.com]

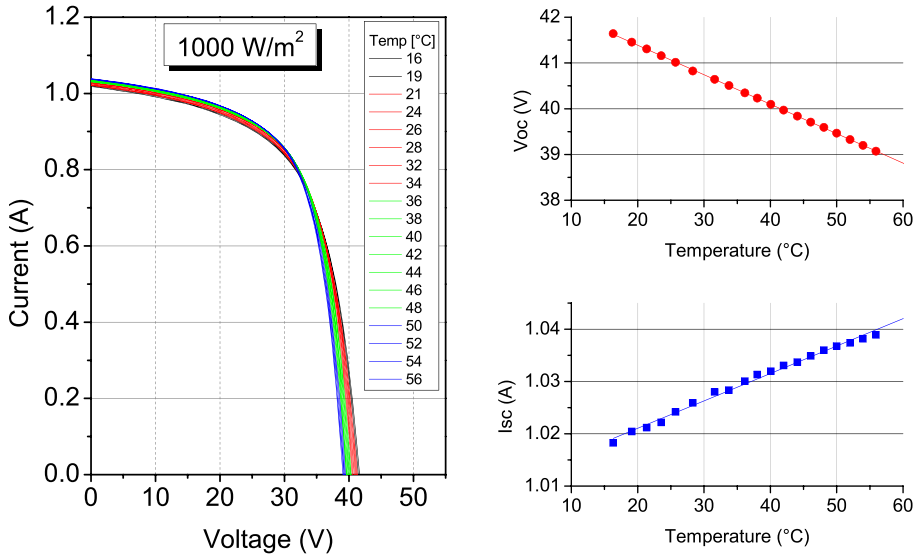

FIGURE 2 I-V curves of the device under test (DUT) measured indoor under simulated sunlight at 1000 W/m^2 and increasing temperature from 15 °C to 55 °C [Colour figure can be viewed at wileyonlinelibrary.com]

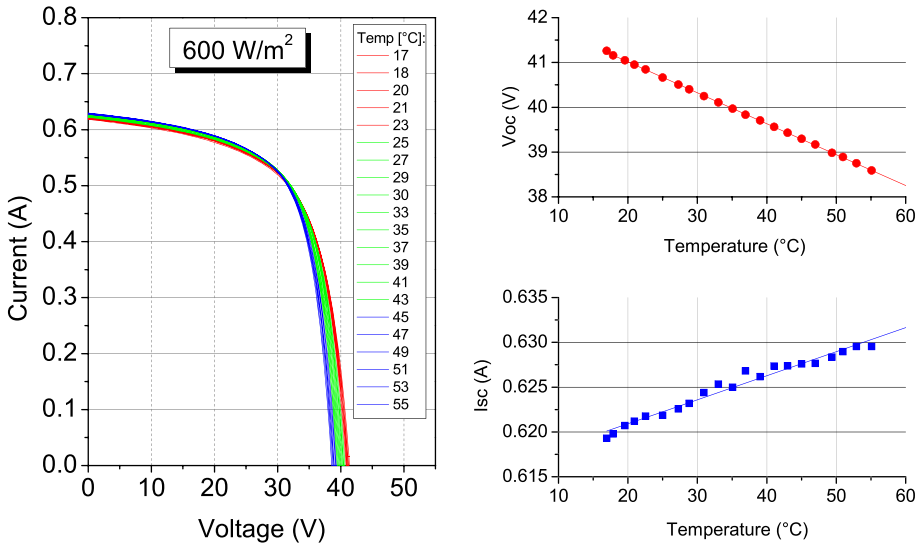

FIGURE 3 I-V curves of the device under test (DUT) measured indoor under simulated sunlight at 600 W/m^2 and increasing temperature from 17 °C to 55 °C [Colour figure can be viewed at wileyonlinelibrary.com]

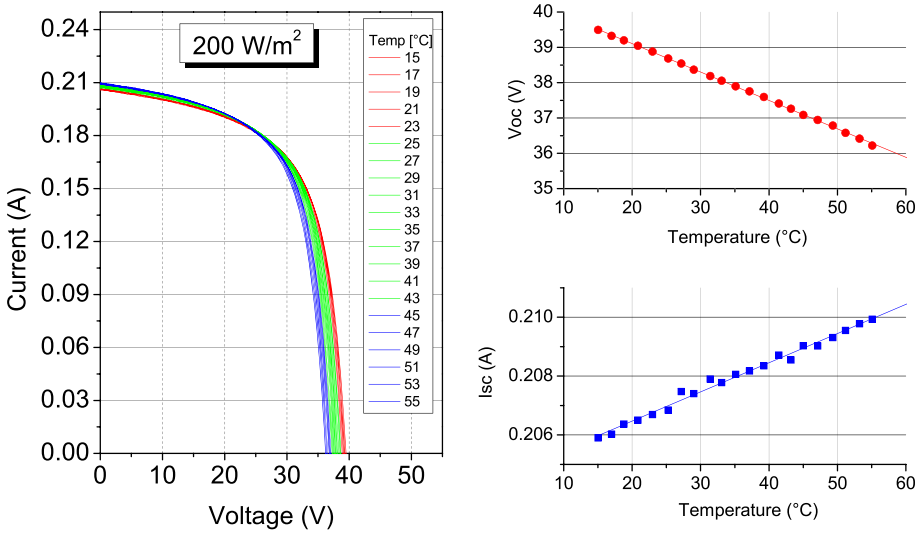

FIGURE 4 I-V curves of the device under test (DUT) measured indoor under simulated sunlight at 200 W/m^2 and increasing temperature from 15 °C to 55 °C [Colour figure can be viewed at wileyonlinelibrary.com]

50 W/m^2. The modules were kept at maximum power condition by an electronic load in the time interval between two measurements. With this method, a long exposure period is required to cover a wide range of the irradiance and temperature conditions required by IEC 61853-1. Furthermore, the measurements are susceptible to angle of incidence and spectral effects during the exposure period. The measurement method is briefly described here. However, the reader can refer to previously published papers[11,12] to have a detailed description and validation of it.

3 | RESULTS

3.1 | Indoor power-matrix measurements

The electrical parameters V_{oc}, I_{sc}, and P_{max} were extracted from the I-V curves and analyzed. The main focus is on the study of the maximum power at various temperature and irradiance combinations (T,G). Figure 1 shows P_{max} data in a surface plot as a function of both temperature and irradiance. The variation of P_{max}(G) in the measured range is obviously strongest, as it can be expected. The overall variation caused by temperature in the range 15 °C to 55 °C at a fixed irradiance is instead only a few percent of it (2% to 4%). For this reason, a plot of P_{max}/irradiance as a function of (T,G) can help enhance the effect of temperature.

In Figures 2–4, all the I-V curves measured at (1000, 600, 200) W/m^2 for all temperatures in the range 15 °C to 55 °C are shown as an example. The variation with temperature of V_{oc} and I_{sc} as extracted from the I-V curves is presented in the insets on the right. Their linear dependence with T is analyzed in more detail, and the results are reported in Table 1. A linear regression as required by IEC 60904-10[5] was used to evaluate the linear dependence of V_{oc} and I_{sc} on T at all irradiance levels, and their relative temperature coefficients α and β were calculated from the slope of the linear fit. The R-square values of the fits were also calculated and give an evaluation of the appropriateness of the linear fit. The maximum permissible value of 5% for deviations of V_{oc}(T) and I_{sc}(T) from the straight-line function[5] was largely satisfied for both I_{sc} and V_{oc} at all irradiance levels. Therefore, it is an acceptable approximation to use linear functions to estimate I_{sc} and V_{oc} values at temperatures different than 25 °C and within the temperature range considered in this study (15 °C to 55 °C). The calculated maximum deviations (Lin max dev) are reported in the last column of the table for each irradiance level.

The calculated α values are comparable at all irradiance levels within their uncertainty and resulted to be in the range [0.042; 0.051]%/°C. This suggests a series of observations and conclusions:

1. I_{sc} linearly increases with temperature within the measured temperature range 15 °C to 55 °C at all irradiance levels within the range [100; 1000] W/m^2. The maximum deviation from linear fit is 0.26%;
2. the value of relative α is not significantly influenced by the irradiance level;
3. the calculated α values differ from those previously reported by other groups[13-15]. However, the actual value can likely depend on the specific device, as already shown for more established technologies like c-Si.[16] Positive α values for OPV devices are usually observed, and this is in agreement to what we report in this study.

Only two groups have measured and reported values for α, to our knowledge. The results are substantially different: Katz et al[17] reported a temperature coefficient α = 0.42 %/°C for a polymer solar cell measured outdoor around 1000 W/m^2, and Krebs et al[14] reported α = 0.003 %/°C for flexible large area roll-to-roll processed polymer solar cell modules measured in a round robin campaign. These very different values, in addition to the one reported in this work, let us think that this coefficient strongly depends on the materials used in the cells and the device structure. Limiting our attention to the DUT of this work, consistent and reproducible data have been found and resulted in the α values reported in Table 1.

The linear negative dependence of V_{oc} with temperature is clearly observed in the measured temperature range at all irradiance levels and suggests the following observations:

1. V_{oc} linearly decreases with temperature;

TABLE 1 Relative α and β for TK801 calculated from the measured I-V curves. The R-square values of the linear regressions as well as the maximum deviations from the linear fit are indicated in the table. The uncertainties (k = 2) of α and β are 0.0072%/°C and 0.0287%/°C, respectively

	I_{sc}			V_{oc}		
Irradiance, W/m^2	α ± 0.0072, %/°C	R^2	Lin max dev	β ± 0.0287, %/°C	R^2	Lin max dev
1000	0.0426	0.989	0.11%	−0.1561	1.000	0.04%
800	0.0506	0.990	0.13%	−0.1600	1.000	0.03%
600	0.0472	0.991	0.11%	−0.1724	1.000	0.08%
400	0.0498	0.955	0.26%	−0.1832	0.999	0.24%
200	0.0479	0.989	0.14%	−0.2080	0.999	0.19%
100	0.0503	0.967	0.20%	−0.2388	0.999	0.20%

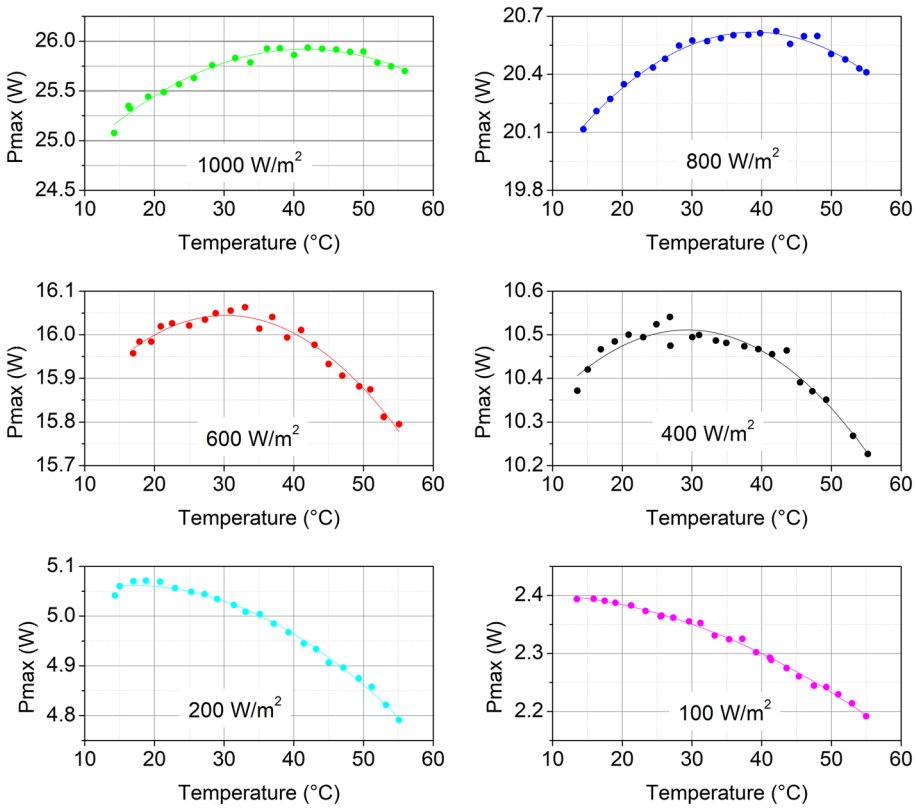

FIGURE 5 Temperature dependence of P_{max} as extracted from the I-V curves, which were measured at different irradiances (1000, 800, 600, 400, 200, 100) W/m^2 and for increasing temperature from about 15 °C to 55 °C. the second-order polynomial fit to the measured data is also shown in the graphs as continuous line [Colour figure can be viewed at wileyonlinelibrary.com]

2. the R^2 values almost close to 1 and the small values of the maximum deviation from the linear fit (below 0.24% at all irradiances) confirm the appropriateness of the linear fit to the data;
3. the calculated β values are in the range [−0.16; −0.24]%/°C and show a progressive increase in absolute terms with lower irradiance levels;
4. these values for β confirm previously measured values by other groups.[14,15]

The variation of P_{max} in the measured range of temperature and irradiance is shown in the surface plots of Figure 1, and its variation with temperature at the different irradiances is reported in Figure 5. Clearly, it cannot be described by a linear function. P_{max} increases with temperature until a certain T, at which it reaches a maximum and finally decreases as T increases. A second-order polynome has been used to fit the data. The polynomial fit is also shown in Figure 5. The parameters calculated from the fit and the R-square values are reported in Table 2. The proposed fit describes satisfactorily the $P_{max}(T)$ dependence. It is interesting to notice that the temperature corresponding to the maximum of $P_{max}(T)$, reported in the last column of the table, constantly shifts to higher values going from low to high irradiance levels. A similar behavior was already observed by us in a previous study on power-matrix measurements of other OPV mini-modules provided to ESTI by a different company. More details about this are reported in Bardizza et al.[18]

On the basis of the polynomial functions whose parameters are reported in Table 2, we calculated P_{max} at nominal temperatures and irradiances to populate the power matrix reported in Table 3.

TABLE 2 Parameters extracted from the second-order polynomial fit to the data of Figure 5. The function has the following equation $y = C + B1x + B2x^2$, and the parameters C, B1, and B2 are reported in the table. The calculated R^2 are included. In the last column, the temperature corresponding to the maximum of P_{max} calculated from the fit is reported

	C		B1		B2		Statistics	Temperature of max from the fit
y = C + B1 x + B2 x ^2	Value	Standard error	Value	Standard error	Value	Standard error	R^2	
P_{max} @1000	24.173	0.071	0.0840	0.0045	−0.00101	0.000064	0.97	41.57
P_{max} @800	19.394	0.034	0.0629	0.0021	−0.00081	0.000029	0.98	38.94
P_{max} @600	15.650	0.031	0.0261	0.0019	−0.00043	0.000026	0.97	30.25
P_{max} @400	10.147	0.033	0.0248	0.0021	−0.00042	0.000031	0.94	29.35
P_{max} @200	5.011	0.012	0.0061	0.0008	−0.00018	0.000011	0.99	16.73
P_{max} @100	2.401	0.007	0.0008	0.0004	−0.00008	0.000006	1.00	4.76

TABLE 3 TK801 power matrix. The P_{max} values were calculated at several nominal temperatures and irradiances by using the polynomial function reported in Table 2

Maximum power—P_{max} [W]									
	Module temperature [°C]								
Irradiance [W/m^2]	15	20	25	30	35	40	45	50	55
100	2.395	2.384	2.369	2.350	2.327	2.300	2.268	2.233	2.193
200	5.061	5.060	5.050	5.030	5.001	4.964	4.917	4.861	4.796
400	10.424	10.474	10.503	10.511	10.498	10.463	10.408	10.331	10.233
600	15.944	15.999	16.033	16.044	16.035	16.004	15.951	15.876	15.780
800	20.155	20.328	20.461	20.554	20.606	20.617	20.588	20.519	20.410
1000	25.205	25.448	25.641	25.783	25.875	25.916	25.906	25.846	25.736

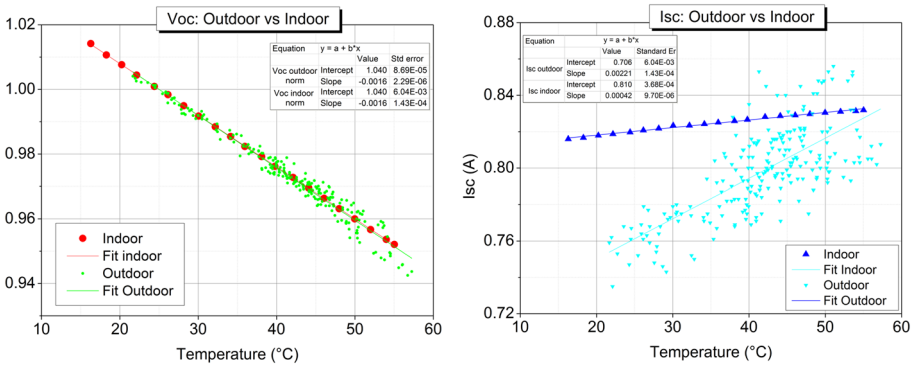

FIGURE 6 Comparison of the temperature dependence of V_{oc} and I_{sc} extracted from I-V curves of the device under test (DUT) measured indoor under solar simulator at 800 W/m^2 and outdoor under natural sunlight in the period august 2018 to June 2019 when the irradiance was in the range (800 ± 5) W/m^2. The V_{oc} data have been normalized to 1 at 25 °C [Colour figure can be viewed at wileyonlinelibrary.com]

3.2 | Outdoor measurements under natural sunlight

After the indoor characterization, the DUT was installed outdoors on ENRA. Data have been acquired since August 2018, and measurements are still running. Preliminary results selected for irradiance within the range (800 ± 5) W/m^2 and based on measurements from the period August 2018 to June 2019 are shown in Figure 6. This irradiance has been selected because of the large number of data available covering almost completely the temperature range 15 °C to 55 °C. The analysis here is focused on the V_{oc} and I_{sc} temperature dependence and on the comparison with the data measured indoor at the solar simulator and described in Section 3.1.

For the scope of this preliminary analysis, the outdoor I-V curves were corrected only to the average irradiance measured during the I-V sweep (sweep time 1 second), while indoor I-V curves are systematically point-by-point corrected for irradiance temporal variations thanks to the simultaneous reading of the reference device. No spectral mismatch correction was applied. I_{sc} and V_{oc} were extracted from the I-V curves by linear fits around V = 0 and I = 0, respectively. In Figure 6, the results for V_{oc} and I_{sc} are shown separately and compared with the results of the power matrix measured indoor. The V_{oc} data were normalized to the value at 25 °C to allow for a better comparison. Linear fits to the measured data (one for indoor and one for outdoor) were done and shown in the graph.

The V_{oc} temperature dependence is clear, and the measurements performed indoor and outdoor replicate the same results. The data in the plot well overlap, and the two linear fits have comparable slope (equal to −0.16%/°C).

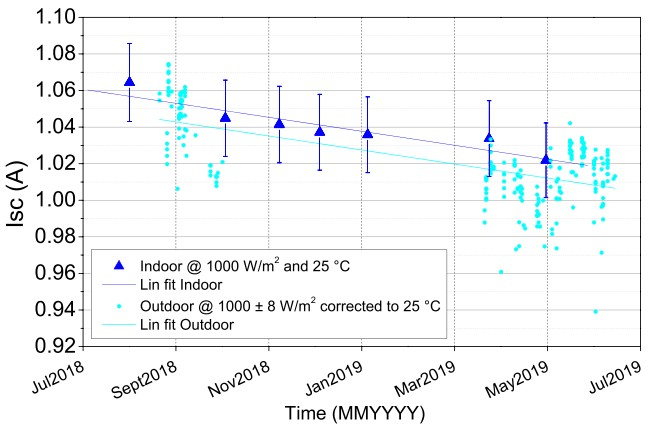

FIGURE 7 Evolution of I_{sc} during 1-year exposure of the device under test (DUT) under natural sunlight. I_{sc} extracted from measurements performed outdoor (corrected to 25 °C) and from periodical check measured indoor show consistently a reduction of about 4 % over the first year [Colour figure can be viewed at wileyonlinelibrary.com]

The case of I_{sc}(T) is more complex, and the preliminary comparison of the results outdoor versus indoor does not show satisfactory agreement. The distribution of the data measured outdoor is wide, and the data are largely disperse. This evident difference can be associated to the following issues:

1. Degradation: a significant degradation of the DUT within the measured period was observed. I_{sc} was the main electrical parameter affected. In Figure 7, the evolution of I_{sc} during the first year of outdoor exposure is shown. In this case, the data have been corrected for temperature to 25 °C by using α temperature coefficient calculated from the power matrix indoor measurements. Periodical I-V measurements were also performed indoor at STC, and the I_{sc} extracted from them is also reported in the graph. A complete analysis of the long-term degradation of the DUT is out of the scope of this article; however, a 4% reduction of I_{sc} from its initial value during the 1-year period was observed for both indoor and outdoor measurements. We expect this to have a significant contribution to the 1-year I_{sc} temperature dependence analysis and consequently to outdoor power-rating measurements of this DUT;
2. Spectral mismatch: as mentioned before, no correction for spectral mismatch was applied in this preliminary study to the outdoor measurements. The spectrum of the sunlight changes considerably during the day and the seasons, especially in the wavelength range for which OPV is responsive. Considering that the in-plane irradiance is measured with a c-Si cell with broad spectral responsivity compared with the DUT, spectral mismatch correction may have a significant impact on I_{sc}.
3. Angle of incidence: DUT is mounted outdoor on a fixed rack facing south. For this reason, the angle of incidence of the light changes continuously. As the analyzed period is relatively long (almost 1 year), the occurrences at which the irradiance was close to 800 W/m^2 may correspond to different angles of incidence. We do not expect this having a large influence on I_{sc} measurements; however, this may also have a small contribution.

4 | CONCLUSIONS

The power-rating measurements of an OPV large-area module performed with a large-area steady-state solar simulator is presented in this paper. Data measured outdoor with the device maintained in real operating conditions were compared with the indoor measurements at controlled conditions. To our knowledge, this is the first case of a power-matrix measurement reported for a large-area OPV commercial full-size module. The results from outdoor systematic monitoring are compared with indoor measurements at controlled conditions.

The temperature dependence of the electrical parameters has been analyzed separately, and our results are consistent and partially confirm previously published literature. The latter is the case of the V_{oc} dependence on T: data measured indoor and outdoor are consistent to each other, confirming the same behavior (linear negative dependence) and resulting in the same β at 800 W/m^2 (−0.16%/°C). Comparable values were observed by us[18] on a different OPV device and by several other groups[14,15,19,20]. The I_{sc} dependence on T seems less systematic in literature, but this can be related to a specific device. The positive linear dependence has been observed at all measured irradiances, and very small (<0.26%) deviations from the straight line were observed. The calculated α are in the range [0.042; 0.051]%/°C at all measured irradiances. The comparison with the measurements performed outdoor is not entirely satisfactory because of three important issues that have not been addressed in this preliminary analysis because of time constraints: medium-term degradation, spectral mismatch correction, and variable angle of incidence. We believe the main contribution is associated to the medium-term degradation, which significantly affects the results. In this study, the device degradation was only partially investigated but still observed through periodic relative I-V measurements carried out indoors. This makes us suggest to carry out initial power-rating measurements indoor under controlled conditions for those devices that are likely to be subject to significant degradation during outdoor exposure.

The variation of P_{max} with temperature at fixed irradiance was fitted with a second-order polynome. At all irradiances, P_{max} increases until a certain temperature is reached (T_{max}), and then it tends to decrease at higher temperatures. The second-order polynomial fit well describes this behavior. Interestingly, the T_{max} value constantly shifts to higher values going from low to high irradiance levels. This behavior (if compared with more established PV technologies[21]) is an unusual characteristic that seems to be specific to OPV devices. It was indeed already observed and qualitatively reported by us and other authors[7,13-15,18] although to our knowledge, it has never been quantified before now.

The data measured so far suggest that for each level of irradiance, there exists a specific temperature at which the power reaches its maximum. Moreover, with increasing irradiance, this "P-optimal temperature" increases. This will be further investigated once more data will be collected.

The results coming out of this work add significant contribution to the OPV technology assessment. The I-V measurements performed here proved to be repeatable and to deliver consistent results.

The analysis on irradiance and temperature dependences presented in this work seems to suggest that OPV devices can work relatively more efficiently than other PV technologies under combined conditions of high irradiance and relatively high temperatures. Indeed, the dependence of P_{max} over T for most established PV technologies (c-Si above all) is well described by a function that is very well approximated by a negative straight line, meaning a constant reduction of the performance (P_{max}) with the increase of temperature. For the OPV case reported here, but also from other previous reported measurements,[6] P_{max}(T) is not described at all by a negative straight line, although it decreases instead of increasing above some temperature threshold that depends on the irradiance. This means, for example, that the relative change of P_{max} at temperatures above the

maximum compared with lower temperatures is significantly lower than for c-Si.

ACKNOWLEDGEMENT

We acknowledge gratefully the help of present and past members of the European Solar Test Installation. In particular, we thank Robert Kenny for the help in setting up the outdoor energy rating measurements and Heinz Ossenbrink for fruitful discussion of the results. Carlos Toledo is grateful to Fundación Séneca - CARM for grant Exp. 19768/FPI/15.

ORCID

Giorgio Bardizza https://orcid.org/0000-0002-1694-5274
Elena Salis https://orcid.org/0000-0002-1273-7638
Carlos Toledo https://orcid.org/0000-0002-4603-6362

REFERENCES

1. Green MA, Hishikawa Y, Dunlop ED, et al. Solar cell efficiency tables (version 53). *Prog Photovolt Res Appl*. 2019;27(1):3-12.
2. IEC 61853-1 Photovoltaic (PV) module performance testing and energy rating—part 1: irradiance and temperature performance measurements and power rating, 2011.
3. Gracia-Amillo A, Bardizza G, Salis E, Huld T, Dunlop ED. Energy-based metric for analysis of organic PV devices in comparison with conventional industrial technologies. *Renew Sustain Energy Rev*. 2018;93:76-89.
4. Carle J, Helgesen M, Hagemann O, et al. Overcoming the scaling lag for polymer solar cells. *Joule*. 2017;1(2):274-289.
5. IEC 60904-10 (Ed.2) Photovoltaic devices—part 10: methods of linearity measurement, International Electrotechnical Commission, 2009.
6. IEC 60904-1 (Ed. 2) Photovoltaic devices—part 1: measurement of photovoltaic current-voltage characteristics, 2006.
7. Bardizza G, Salis E, Pavanello D, Sample T, Müllejans H, Dunlop ED. "Indoor calibration of large area organic PV modules," in Proceedings of the 34th EU PVSEC conference, Bruxelles (Belgium); 2018.
8. IEC 60904-9 (Ed.2) Photovoltaic devices—part 9: solar simulator performance requirements, International Electrotechnical Commission, 2009.
9. Salis E, Sharlandzhiev I. and Field M, "Feasibility study for PV measurements at varying irradiances on a large-area steady-state solar simulator" in *Proceedings of the 33th EU PVSEC conference*, Amsterdam (Netherlands), 2017.
10. Ossenbrink H. and Münzer K. A, "The ESTI sensor—a new reference cell for monitoring of PV plant performance" in *11th European Photovoltaic Solar Energy Conference*, Montreux (Switzerland), 1992.
11. Viganó D, Salis E, Bardizza G, Perin-Gasparin F, Zaaiman W, Müllejans H. and Kenny R. P, "Power rating of photovoltaic modules including validation of procedures to implement IEC 61853-1 on solar simulators and under natural sunlight" in *27th European Photovoltaic Solar Energy Conference*, Frankfurt (Germany), 2012.
12. Kenny RP, Viganó D, Salis E, et al. Power rating of photovoltaic modules including validation of procedures to implement IEC 61853-1 on solar simulators and under natural sunlight. *Prog Photovolt: Res Appl*. 2013;21(6):1384-1399.
13. Bristow N, Kettle J. Outdoor performance of organic photovoltaics: diurnal analysis, dependence on temperature, irradiance and degradation. *Renewable Sustainable Energy*. 2015;7:013111-1 to 013111-12.
14. Krebs FC, Gevorgyan S, et al. A round robin study of flexible large-area roll-to-roll processed polymer solar cell modules. *Solar Energy Materials & Solar Cells*. 2009;93:1968-1977.
15. Katz EA, Faiman D, Tuladhar SM, et al. Temperature dependence for the photovoltaic device parameters of polymer-fullerene solar cells under operating conditions. *J Appl Phys*. 2001;90(10):5343-5350.
16. Salis E, Pavanello D, Kröger I, et al. Results of four European round-robins on short-circuit current temperature coefficient measurements of photovoltaic devices of different size. *Solar Energy*. 2019;179:424-436.
17. Katz E. A, Faiman D, Cohen Y, Padinger F., Brabec C and Sariciftci N. S, "Temperature and irradiance effect on the photovoltaic parameters of a fullerene/conjugated-polymer solar cell" *Proceedings of SPIE—The International Society for Optical Engineering*, p. 4108, 2001.
18. Bardizza G., Salis E, Gracia Amillo A. M, Huld T. and Dunlop E. D, "Power matrix measurements and energy rating analysis of organic PV mini-modules" in *Proceedings of the 33th EU PVSEC conference*, Amsterdam (Netherlands), 2017.
19. Chirvase D, Chiguvare Z, Knipper M, Parisi J, Dyakonov V, Hummelen JC. Temperature dependent characteristics of poly (3 hexylthiophene)-fullerene based heterojunction organic solar cells. *J Appl Phys*. 2003;93(6):3376-3383.
20. Garcia-Belmonte G. Temperature dependence of open-circuit voltage in organic solar cells from generation-recombination kinetic balance. *Solar Energy Materials & Solar Cells*. 2010;94(12):2166-2169.
21. Virtuani A, Rigamonti G, Friesen G, Chianese D. and Beljean P, Fast and accurate methods for the performance testing of highly-efficient c-Si photovoltaic modules using a 10 ms single-pulse solar simulator and customized voltage profiles *Meas Sci Technol*. 2012 vol. 23:115604-1 to 115604-8.

How to cite this article: Bardizza G, Salis E, Toledo C, Dunlop ED. Power performance and thermal operation of organic photovoltaic modules in real operating conditions. *Prog Photovolt Res Appl*. 2020;28:593–600. https://doi.org/10.1002/pip.3234